REPORT 1316

TORSIONAL STIFFNESS OF THIN-WALLED SHELLS HAVING REINFORCING CORES AND RECTANGULAR, TRIANGULAR, OR DIAMOND CROSS SECTION [1]

By HARVEY G. McCOMB, Jr.

SUMMARY

A theoretical investigation has been made of the Saint-Venant torsion of certain composite bars. These bars are composed of two materials—one material in the form of a thin-walled cylindrical shell and the other material in the form of a core which fills the interior of the shell and is bonded to it.

An approximate boundary-value problem is formulated on assumptions similar to those of the theory of torsion of hollow thin-walled shells (Bredt theory). This boundary-value problem is solved exactly for a rectangular cross section and approximately for slender triangular and slender diamond cross sections. Results for the torsional stiffness constants are presented graphically.

INTRODUCTION

Certain airframe components such as wings, stabilizing fins, control surfaces, and helicopter rotor blades have been fabricated by employing a high-strength shell bonded to a core made of some light-weight material. The shell is formed in the external contour of the component and the core fills the interior and acts to stabilize the shell against local buckling. Such a structure has been called a "foam-filled shell" because the core is often a foamed-plastic material. Metal honeycomb and balsa wood have also been used for cores.

A large amount of literature exists on the problem of torsion of homogeneous isotropic cylindrical bars, but relatively little work has been done on the torsion of composite cylinders. A few exact solutions to problems in the torsion of composite sections are presented in references 1 and 2. Solutions for other cross-sectional configurations are desirable, and the methods used in references 1 and 2 do not appear to be applicable for sections of the type considered in the present report.

In this report an approximate boundary-value problem for the torsion of foam-filled shells is formulated. The fact that the thickness of the outer shell is small relative to overall dimensions of the cross section allows an approximation similar to that of the Bredt theory for the torsion of hollow thin-walled shells with free warping. (See ref. 3, pp. 298–302.) For a rectangular cross section, an exact solution to the approximate boundary-value problem is obtained. For slender triangular and slender diamond cross sections, approximate solutions which appear to be reasonably accurate are obtained. Finally, the results are compared with results based on an elementary concept of the torsional stiffness of foam-filled shells.

SYMBOLS

A,B	arbitrary constants
a,b,c	cross-sectional dimensions (see fig. 4)
C	curve defining boundary of a region
$f(\xi),g(\xi)$	arbitrary functions
G_1,G_2	shear moduli of shell and core materials, respectively
$h_n(x)$	Fourier coefficient (see eq. (21))
J_1,J_2	torsional stiffness constants
$K=\frac{G_2 b}{G_1 t}=\frac{G_2 \frac{t_0}{2}}{G_1 t}$	
k_{1n},k_{2n}	arbitrary constants
M	moment on cross section
m	index in equations (37) and (61)
n	summation index
R	region
s	direction tangential to a curve in cross section
t	thickness of shell wall
t_0	dimension of cross section (see fig. 4)
U	total complementary energy per unit length
$\overline{U}=G_2 U$	
x,y,z	coordinates along X-, Y-, and Z-axes, respectively
α_n,β	arbitrary constants
γ	shear strain
$\epsilon=b/a$	
θ	angle of twist per unit length
λ_n	eigenvalues
$\mu=\sqrt{1+\epsilon^2}$	
ν	direction normal to a curve in cross section
ξ,η	nondimensional coordinates in x- and y-directions, respectively
τ	shear stress
ϕ	stress function
Ω	constant of integration

[1] Supersedes NACA Technical Note 3749 by Harvey G. McComb, Jr., 1956.

$\nabla^2 \equiv \frac{\partial^2}{\partial x^2}+\frac{\partial^2}{\partial y^2}$

Subscripts:

1, 2 refer to regions and curves indicated in figure 1

Prime denotes differentiation with respect to the indicated variable.

BASIC EQUATIONS

In this section equations of elasticity are established for the Saint-Venant torsion of certain cylindrical bars composed of two materials. These equations are then particularized to the case of foam-filled thin-walled shells. Finally, the energy approach to the torsion of foam-filled shells is discussed briefly.

TORSION OF CYLINDRICAL BARS CONSISTING OF TWO MATERIALS

Consider a long cylindrical bar composed of two isotropic materials in which one material surrounds the other. A cross section of such a bar is shown in figure 1. For torsion with free warping, the stresses are given in terms of a stress function ϕ as follows:

$$\left.\begin{aligned}\tau_{xz}&=\frac{\partial \phi_i}{\partial y}\\ \tau_{yz}&=-\frac{\partial \phi_i}{\partial x}\end{aligned}\right\} \tag{1}$$

where $i=1$ or 2. Each function ϕ_i must satisfy Poisson's equation

$$\nabla^2\phi_i=-2G_i\theta \tag{2}$$

in its corresponding region R_i.

The boundary conditions can be expressed in terms of the stress function by consideration of the components of shear stress normal and tangential to a curve in the cross section. These components are, respectively,

$$\left.\begin{aligned}\tau_{yz}&=-\frac{\partial \phi}{\partial s}\\ \tau_{zz}&=\frac{\partial \phi}{\partial \nu}\end{aligned}\right\} \tag{3}$$

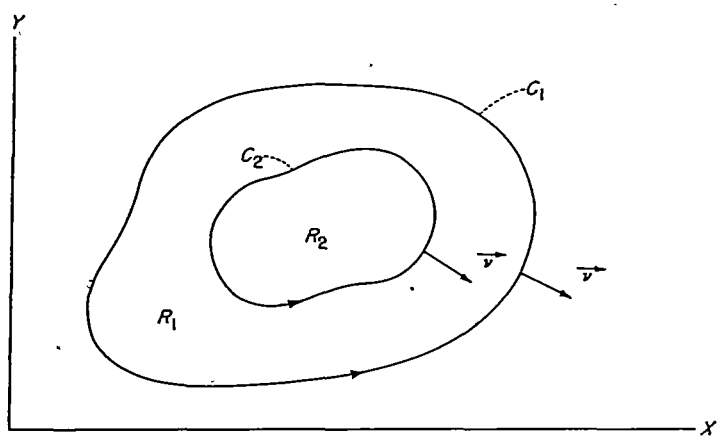

FIGURE 1.—Cross section of cylindrical bar composed of two materials.

The condition that the external boundary of the section must be free of stress is obtained by integrating the first of equations (3) along C_1:

$$\phi_1|_{C_1}=\Omega_1=\text{Constant} \tag{4}$$

The conditions which must be satisfied at the interface C_2 can be seen by referring to figure 2. The tangential strain must be continuous across C_2. In terms of the stress function, this condition is

$$\frac{1}{G_1}\frac{\partial \phi_1}{\partial \nu}\bigg|_{C_2}=\frac{1}{G_2}\frac{\partial \phi_2}{\partial \nu}\bigg|_{C_2} \tag{5}$$

Lastly, the shearing-stress component normal to C_2 must be continuous across C_2, or

$$\frac{\partial \phi_2}{\partial s}\bigg|_{C_2}=\frac{\partial \phi_1}{\partial s}\bigg|_{C_2} \tag{6}$$

When equation (6) is integrated, the following equation results:

$$\phi_2|_{C_2}=\phi_1|_{C_2}+\Omega_2 \tag{7}$$

The problem is to find stress functions ϕ_1 and ϕ_2 which satisfy equation (2) in their respective domains and the boundary conditions (eqs. (4), (5), and (7)).

The total moment on the cross section is given by

$$M=\sum_{i=1}^{2}\iint_{R_i}(\tau_{yz}x-\tau_{xz}y)\,dR_i \tag{8}$$

This equation can be written in terms of ϕ as follows:

$$M=\sum_{i=1}^{2}\iint_{R_i}\left(-x\frac{\partial \phi_i}{\partial x}-y\frac{\partial \phi_i}{\partial y}\right)dx\,dy \tag{9}$$

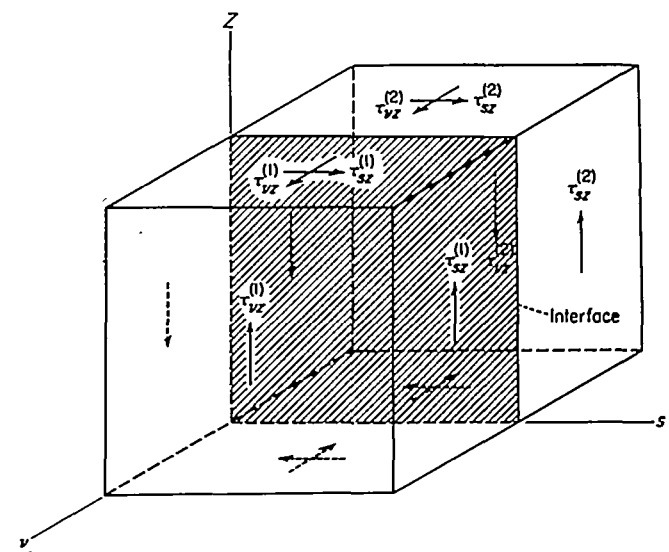

FIGURE 2.—Shearing stresses on an element at the interface between the materials. Superscripts on symbols correspond to regions indicated in figure 1.

Integrating by parts and making use of equations (4) and (7) gives

$$M=\sum_{i=1}^{2}\Omega_i\int_{C_i}(-x\,dy+y\,dx)+\sum_{i=1}^{2}\iint_{R_i}2\phi_i\,dR_i \qquad (10)$$

The stresses and moment on the cross section are independent of Ω_i; therefore, these constants may be chosen arbitrarily. For convenience, Ω_1 and Ω_2 are both taken to be zero so that the expression for the moment is analogous to that for the torsion of a uniform cross section; that is, moment equals twice the volume under the ϕ diagram.

TORSION OF FOAM-FILLED SHELLS

The equations of elasticity are particularized for the case of a cylinder made of a thin-walled shell of one material filled with a core of another, that is, a foam-filled shell. In figure 3 a general cross section for such a cylinder is illustrated. Because the thickness of the shell wall is small compared with the overall dimensions of the cross section, the stress in the wall can be assumed to be uniformly distributed over the thickness. This stress is equal to the normal derivative and is given by

$$\tau_{\text{wall}}=\frac{\partial\phi_1}{\partial\nu}=-\frac{\phi_1}{t}\Big|_{C_2} \qquad (11)$$

where τ_{wall} represents the stress in the shell wall. With the use of equation (11), equations (4), (5), and (7) can now be written as

$$\phi_1|_{C_1}=0 \qquad (12)$$

and

$$\frac{\partial\phi_2}{\partial\nu}\Big|_{C_2}=-\frac{G_2}{G_1}\frac{\phi_1}{t}\Big|_{C_2}=-\frac{G_2}{G_1}\frac{\phi_2}{t}\Big|_{C_2} \qquad (13)$$

Let the curve C in figure 3 be the middle surface of the shell wall. If the shell wall is assumed to be concentrated at its middle surface, then C can be thought of as representing the interface, middle surface, and outer boundary of the wall. Consider R as being the region bounded by C. The problem can now be formulated as follows. Find a function ϕ satisfying the equation

$$\nabla^2\phi=-2G_2\theta \qquad (14)$$

in R and the equation

$$\frac{\partial\phi}{\partial\nu}\Big|_C=-\frac{G_2}{G_1}\frac{\phi}{t}\Big|_C \qquad (15)$$

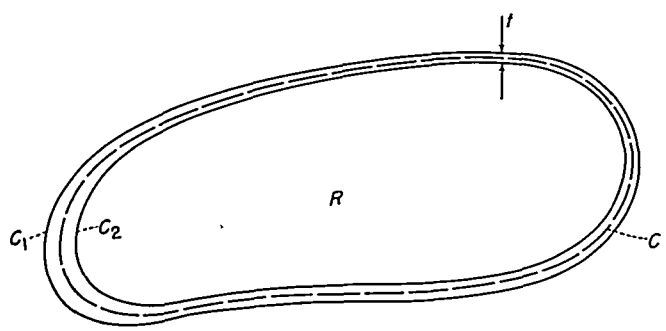

FIGURE 3.—Cross section of a composite thin-walled cylindrical shell.

along C. The moment on the cross section is equal to twice the volume under the ϕ diagram, or

$$M=2\iint_R\phi\,dx\,dy \qquad (16)$$

ENERGY APPROACH

Approximate solutions for the torsion of foam-filled shells can be obtained by the energy method. The complementary energy for such a body is the sum of the stress energy of the core, the stress energy of the shell wall, and the negative of the work done by the external moment acting through the angle of twist. For the composite cross section shown in figure 3 the complementary energy per unit length is

$$U=\frac{1}{2G_2}\iint_R(\tau_{xz}^2+\tau_{yz}^2)dx\,dy+\frac{1}{2G_1}\int_C(\tau_{\text{wall}})^2t\,ds-M\theta \qquad (17)$$

where τ_{xz} and τ_{yz} represent the shear stresses in the core and τ_{wall} represents the shear stress in the shell wall. In terms of the stress function ϕ, U becomes

$$U=\frac{1}{2G_2}\iint_R(\phi_x^2+\phi_y^2-4G_2\theta\phi)dx\,dy+\frac{1}{2G_1}\int_C\phi^2\Big|_C\frac{ds}{t} \qquad (18)$$

where the subscripts on ϕ denote the partial derivative with respect to the indicated variable.

When the variation of U is equated to zero and integrations by parts are carried out, the following equation is obtained:

$$G_2\delta U=0=\int_C\left(\frac{\partial\phi}{\partial\nu}+\frac{G_2}{G_1}\frac{\phi}{t}\right)_C\delta\phi\,ds-\iint_R(\phi_{xx}+\phi_{yy}+2G_2\theta)\delta\phi\,dx\,dy \qquad (19)$$

It is seen that, if $\delta\phi$ is arbitrary in R and along C, equations (14) and (15) must be valid.

The torsion of a foam-filled shell is analogous to the problem of the deflection of a membrane stretched over the region R, subjected to lateral pressure, and supported along the curve C by infinitely many springs which are constrained to distort only in the direction normal to the plane of R. Some discussion of approximate solutions of problems of this type is given in reference 4.

SOLUTION OF SPECIFIC PROBLEMS

In this part of the report an exact solution for a rectangular cross section is obtained by satisfying equations (14) and (15). For the slender triangular and slender diamond cross sections, exact solutions do not appear feasible, and approximate solutions are obtained instead by using equation (18). Two approximate procedures are utilized in each case; the first is the Rayleigh-Ritz method and the second is a more general variational procedure, herein called the "variational method." This latter procedure is applied, for the most part, in cases where the Rayleigh-Ritz method becomes cumbersome. These two approximate methods may be applicable to other sections of practical interest for which solutions are not available.

RECTANGULAR CROSS SECTION

The notation for a rectangular cross section is shown in figure 4 (a). The thickness of the shell wall is assumed to be constant. The problem is to find a function ϕ which satisfies equation (14) within the rectangle and the following boundary conditions:

$$\frac{\partial\phi}{\partial x}=\mp\frac{G_2}{G_1}\frac{\phi}{t} \qquad (at\ x=\pm a) \tag{20a}$$

$$\frac{\partial\phi}{\partial y}=\mp\frac{G_2}{G_1}\frac{\phi}{t} \qquad (at\ y=\pm b) \tag{20b}$$

The function ϕ is, of course, symmetric about both the X- and Y-axes. The symmetry condition about the X-axis is satisfied when ϕ is taken in the form

$$\phi=\sum_{n=0}^{\infty}h_n(x)\cos\lambda_n y \tag{21}$$

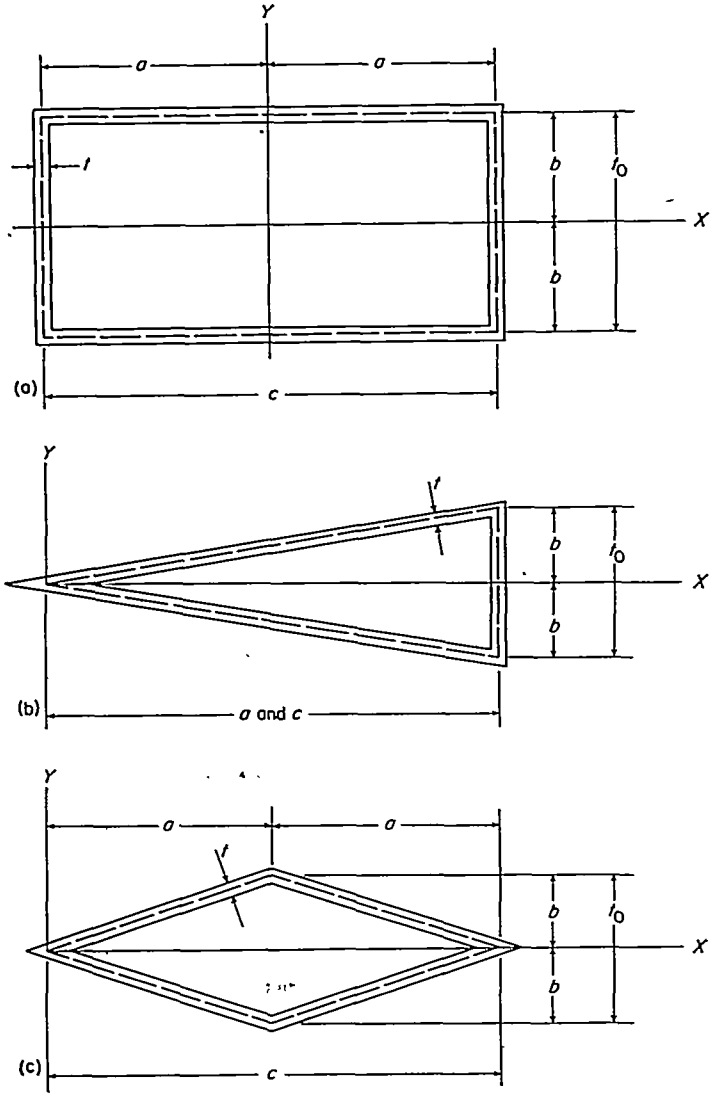

(a) Rectangular cross section.
(b) Triangular cross section.
(c) Diamond cross section.

FIGURE 4.—Notation used in analysis.

where the functions $\cos\lambda_n y$ form an orthogonal set. The right-hand side of equation (14) can be expanded in a Fourier series of the functions $\cos\lambda_n y$ in the interval $-b\leqq y\leqq b$, and this expansion yields

$$\nabla^2\phi=-\sum_{n=0}^{\infty}\frac{4G_2\theta\sin\lambda_n b}{\lambda_n b+\sin\lambda_n b\cos\lambda_n b}\cos\lambda_n y \tag{22}$$

Substituting the assumed solution (eq. (21)) into equation (22) and equating coefficients of like terms gives the following ordinary differential equation for $h_n(x)$:

$$h_n(x)''-\lambda_n^2 h_n(x)=-\frac{4G_2\theta\sin\lambda_n b}{\lambda_n b+\sin\lambda_n b\cos\lambda_n b} \tag{23}$$

The solution to equation (23) is

$$h_n(x)=k_{1n}\sinh\lambda_n x+k_{2n}\cosh\lambda_n x+\frac{4G_2\theta\sin\lambda_n b}{\lambda_n^2(\lambda_n b+\sin\lambda_n b\cos\lambda_n b)} \tag{24}$$

The constants k_{1n} vanish because of symmetry. The constants k_{2n} and the eigenvalues λ_n can be found from the boundary conditions at $x=a$ and $y=b$, respectively. Consider first the condition at $y=b$. The substitution of equation (21) into equation (20b) yields

$$\lambda_n\sin\lambda_n b=\frac{G_2}{G_1 t}\cos\lambda_n b \tag{25}$$

Therefore, the eigenvalues are given by

$$\tan\lambda_n b=\frac{K}{\lambda_n b} \tag{26}$$

where

$$K=\frac{G_2 b}{G_1 t}$$

At $x=a$, the substitution of equation (21) into equation (20a) yields

$$k_{2n}\lambda_n\sinh\lambda_n a=-\frac{G_2}{G_1 t}\left[k_{2n}\cosh\lambda_n a+\frac{4G_2\theta\sin\lambda_n b}{\lambda_n^2(\lambda_n b+\sin\lambda_n b\cos\lambda_n b)}\right] \tag{27}$$

Therefore,

$$k_{2n}=\frac{-4KG_2\theta b^2\sin\lambda_n b}{\lambda_n^2 b^2(\lambda_n b\sinh\lambda_n a+K\cosh\lambda_n a)(\lambda_n b+\sin\lambda_n b\cos\lambda_n b)} \tag{28}$$

Consequently, the stress function is

$$\phi=\sum_{n=0}^{\infty}\frac{4G_2\theta b^2\sin\lambda_n b\cos\lambda_n y}{\lambda_n^2 b^2(\lambda_n b+\sin\lambda_n b\cos\lambda_n b)}\times\left(1-\frac{K\cosh\lambda_n x}{\lambda_n b\sinh\lambda_n a+K\cosh\lambda_n a}\right) \tag{29}$$

The moment on the cross section is given by the formula

$$M=8\int_0^a\int_0^b\phi\,dx\,dy \tag{30}$$

The torsional stiffness can be expressed in terms of either G_1 or G_2

$$\frac{M}{\theta}=G_1J_1=G_2J_2 \tag{31}$$

The torsional stiffness constants J_1 and J_2 are obtained upon substituting equation (29) into equation (30) and carrying out the indicated integration. When the results are expressed in the form of equation (31), it is seen that

$$\left.\begin{aligned} J_1&=4ct_0^2tK\Lambda \\ J_2&=2ct_0^3\Lambda \end{aligned}\right\} \tag{32}$$

where

$$\Lambda=\sum_{n=0}^{\infty}\frac{\sin^2\lambda_nb}{\lambda_n^3b^3(\lambda_nb+\sin\lambda_nb\cos\lambda_nb)}\times \left[1-\frac{b}{a}\frac{K\sinh\lambda_na}{\lambda_nb(\lambda_nb\sinh\lambda_na+K\cosh\lambda_na)}\right] \tag{33}$$

The series Λ converges very rapidly. For various values of K, the eigenvalues are easily located from the intersections of the hyperbola K/λ_nb and the curves $\tan\lambda_nb$ as indicated in figure 5. Plots of J_1 and J_2 against the cross-section aspect ratio t_0/c for various values of K are presented in figure 6.

As the stiffness of the shell-wall material vanishes, K approaches infinity and λ_nb approaches $\frac{(2n+1)\pi}{2}$. It can be shown that the limiting value of J_2 is the solution obtained by the theory of elasticity for the torsion of a homogeneous rectangular cross section as given in reference 3 (p. 278).

As the stiffness of the core material vanishes, K approaches zero and the solution should approach that of the Bredt theory for the torsion of hollow thin-walled shells with free warping. As K approaches zero, λ_nb approaches $n\pi$. It is obvious, then, that all the terms in Λ vanish for which $n>0$. Investigation of the term for which $n=0$ shows that J_1 does approach the result given by the Bredt theory which is

$$\lim_{K\to 0}J_1=\frac{4A_0^2}{\oint\frac{ds}{t}}=\frac{2ct_0^2t}{\left(1+\frac{t_0}{c}\right)} \tag{34}$$

where A_0 is the area enclosed by the median line of the shell wall.

SLENDER TRIANGULAR CROSS SECTION

If the energy approach is used, two approximate solutions are obtained for a cross section in the shape of a slender isosceles triangle with a constant-thickness shell wall as illustrated in figure 4 (b). One solution is obtained by the Rayleigh-Ritz method and another solution is found by utilizing the calculus of variations and the boundary-layer technique of reference 5.

Rayleigh-Ritz method.—In terms of nondimensional coordinates, the complementary energy (eq. (18)) can be written for the triangle as follows:

$$\begin{aligned}\overline{U}&=G_2U \\ &=\int_0^1\int_0^{\xi}(\epsilon^2\phi_\xi^2+\phi_\eta^2-4G_2\theta b^2\phi)\frac{1}{\epsilon}d\eta\,d\xi+\frac{K\mu}{\epsilon}\int_0^1\phi^2\Big|_{\eta=\xi}d\xi+ \\ &\qquad K\int_0^1\phi^2\Big|_{\xi=1}d\eta\end{aligned} \tag{35}$$

where

$$\xi=\frac{x}{a}\qquad \eta=\frac{y}{b}\qquad \epsilon=\frac{b}{a}\qquad \mu=\sqrt{1+\epsilon^2}$$

Note that the equation of the sloping side of the triangle in nondimensional coordinates is simply $\eta=\xi$.

The stress function ϕ must be an even function through the thickness, and for slender sections it is usually sufficient to assume a parabolic variation in the thickness direction.

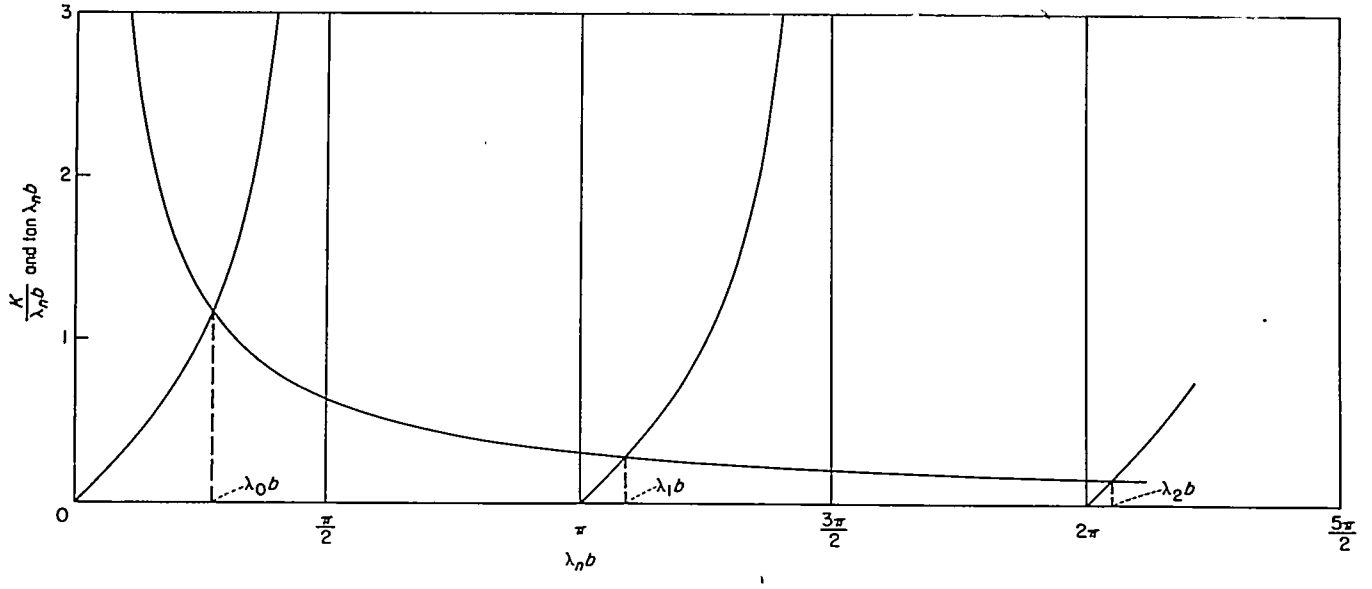

FIGURE 5.—Determination of eigenvalues in exact solution for rectangular cross section.

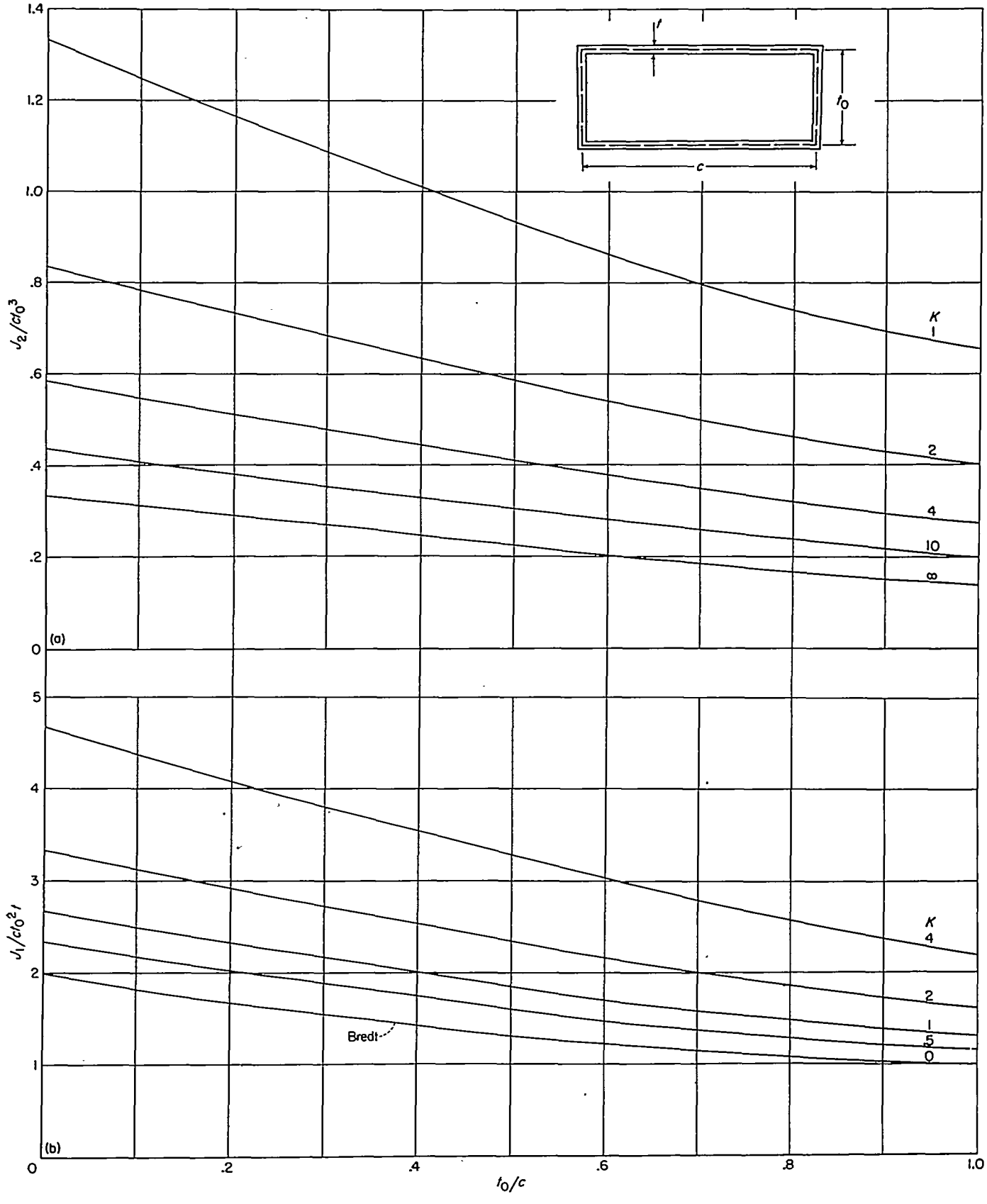

(a) Constant associated with shear modulus of core material.
(b) Constant associated with shear modulus of shell-wall material.

FIGURE 6.—Torsional stiffness constants for a composite thin-walled cylindrical shell of rectangular cross section.

$$M/\theta = G_1J_1 = G_2J_2;\ K = \frac{G_2\frac{t_0}{2}}{G_1t}$$

For thick sections, however, it may be necessary to include additional terms in the thickness direction to get satisfactory accuracy. Suppose now that ϕ is assumed to be a polynomial

$$\phi=\sum_{n=0}^{r}\alpha_n\xi^n+\beta\eta^2 \tag{36}$$

When equation (36) is substituted into equation (35) and $\overline{U}$ is minimized with respect to the parameters α_m and β, the following $r+2$ equations result:

$$\left.\begin{aligned}&\frac{\partial\overline{U}}{\partial\alpha_m}=0\\&=\sum_{n=0}^{r}\alpha_n\left(\epsilon^2\frac{mn}{m+n}+\frac{K\mu}{m+n+1}+K\epsilon\right)+\beta\left(\frac{K\mu}{m+3}+\frac{K\epsilon}{3}\right)-\frac{2}{m+2}G_2\theta b^2\\&\frac{\partial\overline{U}}{\partial\beta}=0\\&=\sum_{n=0}^{r}\alpha_n\left(\frac{K\mu}{n+3}+\frac{K\epsilon}{3}\right)+\beta\left(\frac{K\mu}{5}+\frac{K\epsilon}{5}+\frac{1}{3}\right)-\frac{1}{6}G_2\theta b^2\end{aligned}\right\} \tag{37}$$

where $0\leqq m\leqq r$.

Solution of the system of simultaneous equations (37) yields α_n and β. From equation (16), the moment is

$$M=ab\left(4\sum_{n=0}^{r}\frac{\alpha_n}{n+2}+\frac{\beta}{3}\right) \tag{38}$$

The stiffness can be written in the form of equation (31) and J_1 and J_2 are easily calculated. The results are

$$\left.\begin{aligned}J_1&=\frac{ctt_0^2}{12}K\left(12\sum_{n=0}^{r}\frac{1}{n+2}\frac{\alpha_n}{G_2\theta b^2}+\frac{\beta}{G_2\theta b^2}\right)\\J_2&=\frac{ct_0^3}{12}\left(6\sum_{n=0}^{r}\frac{1}{n+2}\frac{\alpha_n}{G_2\theta b^2}+\frac{\beta}{2G_2\theta b^2}\right)\end{aligned}\right\} \tag{39}$$

When K is large compared with unity a large number of equations may be required for reasonable accuracy. An approach which avoids this difficulty is developed in the succeeding section.

Variational method.—Instead of assuming for ϕ the polynomial of equation (36), suppose arbitrary functions of ξ are allowed to remain and ϕ is taken to be of the form

$$\phi=f(\xi)+\eta^2g(\xi) \tag{40}$$

When equation (40) is substituted into equation (35) and the variation of $\overline{U}$ with respect to admissible variations in f and g is equated to zero, two simultaneous ordinary differential equations for the functions f and g are obtained as follows:

$$\left.\begin{aligned}&\epsilon^2(\xi f')'+\frac{\epsilon^2}{3}(\xi^3g')'-K\mu(f+\xi^2g)=-2G_2\theta b^2\xi\\&\frac{\epsilon^2}{3}(\xi^3f')'+\frac{\epsilon^2}{5}(\xi^5g')'-K\mu(\xi^2f+\xi^4g)-\frac{4}{3}\xi^3g=-\frac{2}{3}G_2\theta b^2\xi^3\end{aligned}\right\} \tag{41}$$

and the following boundary conditions are obtained:

$$\left(\xi f'+\frac{\xi^3}{3}g'\right)_{\xi\to0}=0 \tag{42a}$$

$$\left(\xi^3f'+\frac{3}{5}\xi^5g'\right)_{\xi\to0}=0 \tag{42b}$$

$$(\epsilon f'+Kf)_{\xi=1}=0 \tag{42c}$$

$$(\epsilon g'+Kg)_{\xi=1}=0 \tag{42d}$$

where the primes denote derivatives with respect to ξ.

The differential equations (41) are linear with variable coefficients, and it appears to be a difficult task to find an exact solution to the system. For the case of slender cross sections, however, an approximate solution is possible by utilizing the "boundary layer" technique discussed in reference 5. Notice that the differentiated terms in equations (41) are multiplied by ϵ^2, a quantity which for slender cross sections is small compared with unity. Differential equations having the most highly differentiated terms multiplied by a small quantity are characteristic of the type of boundary-layer problems considered in reference 5.

Suppose, initially, that f and g are slowly varying functions throughout the region $0\leqq\xi\leqq1$. The term "slowly varying" is intended to mean that the maximum values of the functions f and g and their derivatives which appear in equations (41) are of the same order of magnitude. Then, as long as K is at least of the order of unity, the terms in equations (41) which contain ϵ^2 have little influence on the solution. Consequently, a good approximation to a particular solution is obtained by ignoring the terms in equations (41) which contain ϵ^2.

When this procedure is carried out, it is found that the approximate particular solution satisfies the boundary conditions at $\xi=0$ but does not satisfy the boundary conditions at $\xi=1$. It can be concluded that the required solution is such that the functions f and g are not slowly varying everywhere in the region $0\leqq\xi\leqq1$. Somewhere the derivatives which appear in equations (41) must take on values which are of the order of ϵ^{-2} so that the terms containing ϵ^2 can have an appreciable influence on the solution.

It is assumed that the region where the derivatives of f and g have values of the order of ϵ^{-2} is confined to a so-called boundary layer in the neighborhood of $\xi=1$. On the basis of this assumption, the particular solution alone is a good approximation to the exact solution away from $\xi=1$. Then, by focusing attention on the boundary layer close to $\xi=1$, it is possible to obtain an approximate homogeneous solution to equations (41) which modifies the particular solution in such a manner that the boundary conditions at $\xi=1$ can be satisfied.

It is convenient to get a particular solution as a power series in ϵ instead of ignoring completely the ϵ^2 terms in equations (41). Assume that a solution can be expressed in the form

$$\left.\begin{aligned}f_P(\xi)&=f_{P0}(\xi)+\epsilon f_{P1}(\xi)+\epsilon^2f_{P2}(\xi)+\ \cdots\\g_P(\xi)&=g_{P0}(\xi)+\epsilon g_{P1}(\xi)+\epsilon^2g_{P2}(\xi)+\ \cdots\end{aligned}\right\} \tag{43}$$

where the subscript P denotes a particular solution. When equations (43) are substituted into equations (41) and coefficients of like powers of ϵ are equated, pairs of simultaneous equations are obtained for the coefficients in the power series. For example, when the coefficients of the zeroeth power of ϵ are equated there results

$$\left.\begin{aligned} K\mu(f_{P0}+\xi^2 g_{P0})&=2G_2\theta b^2\xi \\ K\mu(f_{P0}+\xi^2 g_{P0})+\frac{4}{3}\xi g_{P0}&=\frac{2}{3}G_2\theta b^2\xi \end{aligned}\right\} \tag{44a}$$

When coefficients of the first power of ϵ are equated the result is

$$\left.\begin{aligned} f_{P1}+\xi^2 g_{P1}&=0 \\ K\mu(f_{P1}+\xi^2 g_{P1})+\frac{4}{3}\xi g_{P1}&=0 \end{aligned}\right\} \tag{44b}$$

When coefficients of the second power of ϵ are equated the following equations result:

$$\left.\begin{aligned} (\xi f_{P0}')'+\frac{1}{3}(\xi^3 g_{P0}')'-K\mu(f_{P2}+\xi^2 g_{P2})&=0 \\ \frac{1}{3}(\xi^3 f_{P0}')'+\frac{1}{5}(\xi^5 g_{P0}')'-K\mu(\xi^2 f_{P2}+\xi^4 g_{P2})-\frac{4}{3}\xi^3 g_{P2}&=0 \end{aligned}\right\} \tag{44c}$$

Similar equations are obtained when coefficients of higher powers of ϵ are equated.

Solution of equations (44) results in the following expressions for f_P and g_P:

$$\left.\begin{aligned} f_P&=G_2\theta b^2\left[\frac{2\xi}{K\mu}+\xi^2+\epsilon^2\left(\frac{2}{K^2\mu^2}+\frac{4\xi}{K\mu}+\xi^2\right)+\cdots\right] \\ g_P&=-G_2\theta b^2(1+\epsilon^2+\cdots) \end{aligned}\right\} \tag{45}$$

Coefficients of the odd powers of ϵ vanish. This particular solution satisfies the boundary conditions at $\xi=0$ but not at $\xi=1$.

A homogeneous solution can be obtained which modifies the particular solution in the vicinity of $\xi=1$ in such a way that the boundary conditions at $\xi=1$ can be satisfied. In order to determine the homogeneous solution it is convenient to put equations (41) into a form in which, in the neighborhood of $\xi=1$, the terms containing derivatives are of the same order of magnitude as the remaining terms. Such a conversion is provided by the coordinate transformation

$$\xi=1+\epsilon\bar{\xi} \tag{46}$$

When the transformation (eq. (46)) is introduced into equations (41) and the right-hand sides are set equal to zero, the following equations are obtained:

$$\left.\begin{aligned} &[(1+\epsilon\bar{\xi})f']'+\frac{1}{3}[(1+\epsilon\bar{\xi})^3 g']'-K\mu[f+(1+\epsilon\bar{\xi})^2 g]=0 \\ &\frac{1}{3}[(1+\epsilon\bar{\xi})^3 f']'+\frac{1}{5}[(1+\epsilon\bar{\xi})^5 g']'-K\mu[(1+\epsilon\bar{\xi})^2 f+ \\ &\qquad (1+\epsilon\bar{\xi})^4 g]-\frac{4}{3}(1+\epsilon\bar{\xi})^3 g=0 \end{aligned}\right\} \tag{47}$$

where the primes now denote differentiation with respect to $\bar{\xi}$.

The homogeneous solution can be expanded in powers of ϵ

$$\left.\begin{aligned} f_H(\bar{\xi})&=f_{H0}(\bar{\xi})+\epsilon f_{H1}(\bar{\xi})+\epsilon^2 f_{H2}(\bar{\xi})+\cdots \\ g_H(\bar{\xi})&=g_{H0}(\bar{\xi})+\epsilon g_{H1}(\bar{\xi})+\epsilon^2 g_{H2}(\bar{\xi})+\cdots \end{aligned}\right\} \tag{48}$$

where the subscript H denotes a homogeneous solution. If these expressions are substituted into equations (47) and the coefficients of like powers of ϵ are equated, systems of ordinary differential equations are obtained. For the terms f_{H0} and g_{H0}, a set of homogeneous equations is obtained:

$$\left.\begin{aligned} f_{H0}''+\frac{1}{3}g_{H0}''-K\mu(f_{H0}+g_{H0})&=0 \\ \frac{1}{3}f_{H0}''+\frac{1}{5}g_{H0}''-K\mu(f_{H0}+g_{H0})-\frac{4}{3}g_{H0}&=0 \end{aligned}\right\} \tag{49}$$

For the terms f_{H1} and g_{H1} the following nonhomogeneous equations are obtained:

$$\left.\begin{aligned} f_{H1}''+\frac{1}{3}g_{H1}''-K\mu(f_{H1}+g_{H1})&=-(\bar{\xi}f_{H0}')'-(\bar{\xi}g_{H0}')'+ \\ &\qquad 2K\mu\bar{\xi}g_{H0} \\ \frac{1}{3}f_{H1}''+\frac{1}{5}g_{H1}''-K\mu(f_{H1}+g_{H1})-\frac{4}{3}g_{H1}&=-(\bar{\xi}f_{H0}')'- \\ &\qquad (\bar{\xi}g_{H0}')'+2K\mu\bar{\xi}(f_{H0}+2g_{H0})+4\bar{\xi}g_{H0} \end{aligned}\right\} \tag{50}$$

Additional sets of nonhomogeneous equations would result for the coefficients of higher order terms.

It is found that neglecting terms of the order of ϵ in equations (48) is equivalent to neglecting terms only of the order of ϵ^2 in the final result for the torsional stiffness constants. Therefore, a final result which includes all terms linear in ϵ can be obtained by solving only equations (49) and dropping all higher order terms in the homogeneous solution. Solutions to equations (49) are of the form

$$f_{H0}=Ae^{\lambda\bar{\xi}}$$

$$g_{H0}=Be^{\lambda\bar{\xi}}$$

Substitution of these functions into equations (49) yields

$$\left.\begin{aligned} A(\lambda^2-K\mu)+B\left(\frac{\lambda^2}{3}-K\mu\right)&=0 \\ A\left(\frac{\lambda^2}{3}-K\mu\right)+B\left(\frac{\lambda^2}{5}-K\mu-\frac{4}{3}\right)&=0 \end{aligned}\right\} \tag{51}$$

This system of equations has a solution only if the determinant of the coefficients vanishes. When the determinant is set equal to zero a biquadratic equation for λ is obtained. The solution to the biquadratic equation is

$$\lambda=\pm\sqrt{\frac{15+6K\mu\pm\sqrt{(15+6K\mu)^2-60K\mu}}{2}} \tag{52}$$

The homogeneous solution must vanish as the absolute magnitude of $\bar{\xi}$ increases, and since $\bar{\xi}$ is always negative or zero, only the two positive roots for λ are required.

From the first of equations (51) the B coefficients can be written in terms of the A coefficients

$$B=-3\,\frac{\lambda^2-K\mu}{\lambda^2-3K\mu}\,A \tag{53}$$

When the $\bar{\xi}$ coordinate is transformed to the ξ coordinate and terms of the order of ϵ^2 are dropped, an approximate general solution to equations (41) is obtained

$$\left.\begin{aligned} f&=\sum_{n=1}^{2} A_n e^{-\frac{\lambda_n}{\epsilon}\frac{\lambda_n}{\epsilon}\xi}+G_2\theta b^2\left(\frac{2\xi}{K\mu}+\xi^2\right) \\ g&=-\sum_{n=1}^{2} 3\,\frac{\lambda_n^2-K\mu}{\lambda_n^2-3K\mu}\,A_n e^{-\frac{\lambda_n}{\epsilon}\frac{\lambda_n}{\epsilon}\xi}-G_2\theta b^2 \end{aligned}\right\} \tag{54}$$

This solution satisfies the boundary conditions at $\xi=0$. The boundary conditions at $\xi=1$ are used to determine A_1 and A_2.

When equations (54) are used, the stress function ϕ becomes

$$\phi=G_2\theta b^2\left[\sum_{n=1}^{2}\overline{A}_n\left(1-3\,\frac{\lambda_n^2-K\mu}{\lambda_n^2-3K\mu}\,\eta^2\right)e^{-\frac{\lambda_n}{\epsilon}\frac{\lambda_n}{\epsilon}\xi}+\frac{2\xi}{K\mu}+\xi^2-\eta^2\right] \tag{55}$$

where

$$\overline{A}_n=\frac{A_n}{G_2\theta b^2}$$

and where terms of the order of ϵ^2 are dropped. The moment is calculated by substituting ϕ into equation (16) and performing the integration. The results for the torsional stiffness constants J_1 and J_2 are

$$\left.\begin{aligned} J_1&=\frac{ct_0^2t}{12}\,2K\Gamma \\ J_2&=\frac{ct_0^3}{12}\,\Gamma \end{aligned}\right\} \tag{56}$$

where

$$\Gamma=1+\frac{4}{K\mu}+6\sum_{n=1}^{2}\overline{A}_n\,\frac{\epsilon}{\lambda_n}\left(\frac{-2K\mu}{\lambda_n^2-3K\mu}\right) \tag{57}$$

and where terms of the order of ϵ^2 have been dropped. It is seen now that in calculating the arbitrary constants $\overline{A}_n$, terms of the order of ϵ may be neglected. When equations (54) are substituted into the boundary conditions (eqs. (42c) and (42d)) the following expressions for $\overline{A}_n$ are obtained after dropping terms of the order of ϵ:

$$\left.\begin{aligned} \overline{A}_1&=\frac{\left(\frac{2}{\mu}+K\right)\lambda_2^2-2K}{(\lambda_1+K)\sqrt{(15+6K\mu)^2-60K\mu}} \\ \overline{A}_2&=-\frac{\left(\frac{2}{\mu}+K\right)\lambda_1^2-2K}{(\lambda_2+K)\sqrt{(15+6K\mu)^2-60K\mu}} \end{aligned}\right\} \tag{58}$$

In the limiting case where K approaches zero the boundary-layer technique becomes invalid. Therefore, the solution cannot be expected to approach the proper result for a hollow thin-walled shell. When K approaches infinity, an approximate solution for a solid cross section is obtained; and Γ is given by

$$\lim_{K\to\infty}\Gamma=1-4\sqrt{\frac{2}{5}}\,\epsilon \tag{59}$$

SLENDER DIAMOND CROSS SECTION

Rayleigh-Ritz method.—For the slender diamond cross section the notation is shown in figure 4 (c). The complementary energy becomes

$$\overline{U}=2\int_0^1\int_0^{\xi}\left(\epsilon^2\phi_\xi^2+\phi_\eta^2-4G_2\theta b^2\phi\right)\frac{1}{\epsilon}\,d\eta\,d\xi+2\,\frac{K\mu}{\epsilon}\int_0^1\phi^2\Big|_{\eta=\xi}d\xi \tag{60}$$

Substitution of the polynomial (eq. (36)) into equation (60) and minimization with respect to α_m and β yields the $r+2$ equations

$$\left.\begin{aligned} \frac{\partial\overline{U}}{\partial\alpha_m}=0&=\sum_{n=0}^{r}\alpha_n\left(\epsilon^2\,\frac{mn}{m+n}+\frac{K\mu}{m+n+1}\right)+\beta\,\frac{K\mu}{m+3}-\frac{2}{m+2}\,G_2\theta b^2 \\ \frac{\partial\overline{U}}{\partial\beta}=0&=\sum_{n=0}^{r}\alpha_n\,\frac{K\mu}{n+3}+\beta\left(\frac{K\mu}{5}+\frac{1}{3}\right)-\frac{1}{6}\,G_2\theta b^2 \end{aligned}\right\} \tag{61}$$

where $0\leqq m\leqq r$.

The moment and the torsional stiffness constants J_1 and J_2 are found by utilizing equation (16). The expressions for the torsional stiffness constants turn out to be precisely the same as for the triangular cross section given in equations (39). Of course, for the diamond cross section, α_n and β are obtained from equations (61).

Variational method.—Through the use of the calculus of variations and expression (40) for ϕ, the differential equations (41) are found to be valid also for the diamond cross section. The boundary equations at $\xi=0$ (eqs. (42a) and (42b)) also

hold for the diamond cross section. The boundary conditions at $\xi=1$, however, are now given by

$$\left.\begin{aligned} f'|_{\xi=1}&=0\\ g'|_{\xi=1}&=0 \end{aligned}\right\} \tag{62}$$

where the primes denote differentiation with respect to ξ.

The boundary-layer technique yields a general solution of the same form as that obtained for the triangle. However, now it is found that neglecting terms of the order of ϵ in the homogeneous solution (eqs. (48)) is equivalent to neglecting terms only of the order of ϵ^3 in the final expressions for the torsional stiffness constants. Consequently, for the diamond cross section a result which includes all terms of the order of ϵ^2 can be obtained by solving equations (49) and dropping all higher order terms in the homogeneous solution. It is consistent, now, to keep the ϵ^2 term in the particular solution.

The approximate general solution to equations (41) for the diamond cross section becomes

$$\left.\begin{aligned} f&=\sum_{n=1}^{2} A_n e^{\frac{\lambda_n}{\epsilon}\frac{\lambda_n}{\epsilon}\xi}+G_2\theta b^2\left[\frac{2\xi}{K\mu}+\xi^2+\epsilon^2\left(\frac{2}{K^2\mu^2}+\frac{4\xi}{K\mu}+\xi^2\right)\right]\\ g&=-\sum_{n=1}^{2} 3\frac{\lambda_n^2-K\mu}{\lambda_n^2-3K\mu}A_n e^{\frac{\lambda_n}{\epsilon}\frac{\lambda_n}{\epsilon}\xi}-G_2\theta b^2(1+\epsilon^2) \end{aligned}\right\} \tag{63}$$

The arbitrary constants A_1 and A_2 are determined by substituting equations (63) into equations (62).

The stress function becomes

$$\phi=G_2\theta b^2\left[\sum_{n=1}^{2}\overline{A}_n\left(1-3\frac{\lambda_n^2-K\mu}{\lambda_n^2-3K\mu}\eta^2\right)e^{\frac{\lambda_n}{\epsilon}\frac{\lambda_n}{\epsilon}\xi}+\frac{2\xi}{K\mu}+\xi^2-\eta^2+\epsilon^2\left(\frac{2}{K^2\mu^2}+\frac{4\xi}{K\mu}+\xi^2-\eta^2\right)\right] \tag{64}$$

If this expression for ϕ is substituted into equation (16) and integrated, the moment can be calculated. The torsional stiffness constants become

$$\left.\begin{aligned} J_1&=\frac{ct_0^2t}{12}2K\Gamma^*\\ J_2&=\frac{ct_0^3}{12}\Gamma^* \end{aligned}\right\} \tag{65}$$

where

$$\Gamma^*=1+\frac{4}{K\mu}+\epsilon^2\left(\frac{6}{K^2\mu^2}+\frac{8}{K\mu}+1\right)+6\sum_{n=1}^{2}\overline{A}_n\frac{\epsilon}{\lambda_n}\left(\frac{-2K\mu}{\lambda_n^2-3K\mu}\right) \tag{66}$$

When equations (63) are substituted into the boundary conditions (eqs. (62)) and terms of the order of ϵ^2 are neglected, the following expressions are obtained for the arbitrary constants:

$$\left.\begin{aligned} \overline{A}_1&=\epsilon\frac{1+K\mu}{K\mu}\frac{2\lambda_2^2+3K\mu}{\lambda_1\sqrt{(15+6K\mu)^2-60K\mu}}\\ \overline{A}_2&=-\epsilon\frac{1+K\mu}{K\mu}\frac{2\lambda_1^2+3K\mu}{\lambda_2\sqrt{(15+6K\mu)^2-60K\mu}} \end{aligned}\right\} \tag{67}$$

In the case where K approaches infinity an approximate solution for a solid section is obtained, and Γ^* is given by

$$\lim_{K\to\infty}\Gamma^*=1-3\epsilon^2 \tag{68}$$

RESULTS AND DISCUSSION

PRESENTATION OF RESULTS

The results of the calculations outlined in this report are presented in figures 6, 7, and 8. These figures show plots of the torsional stiffness constants against cross-section aspect ratio for various values of the parameter K. The torsional stiffness can be expressed either in terms of the shear modulus of the core material or the shear modulus of the shell-wall material. The torsional stiffness constant associated with the shear modulus of the core material J_2 is plotted in parts (a) of figures 6, 7, and 8, whereas the constant associated with the shear modulus of the shell-wall material J_1 is plotted in parts (b) of these figures.

In figure 6 are shown the results of the exact solution of the differential equation (14) with the boundary conditions (20) for a rectangular cross section. In figures 7 and 8 are shown the results of the approximate solutions (the Rayleigh-Ritz method and the variational method in conjunction with the boundary-layer technique) for the triangular and diamond cross sections. A five parameter polynomial was used in the Rayleigh-Ritz method.

ACCURACY OF APPROXIMATE METHODS

Solutions by the Rayleigh-Ritz and variational methods also were obtained for the rectangular cross section. A comparison of these results with the exact solution provides an indication of the accuracy of the approximate methods.

A polynomial with only three parameters was used for the Rayleigh-Ritz method in this comparison. The results showed that for all aspect ratios and for K less than about unity the stiffness given by Rayleigh-Ritz method is less than 3 percent lower than the exact stiffness. It is believed that the five-parameter Rayleigh-Ritz method used for the triangular and diamond cross sections should yield slightly more accurate results. Of course the accuracy of the Rayleigh-Ritz method can be improved for large values of K by including more terms in the polynomial for ϕ. However, the number of simultaneous equations which must be solved increases with the number of unknown parameters.

The stiffness calculated by the variational method for the rectangular cross section was less than 1 percent in error for values of K greater than about unity and the aspect ratio t_0/c less than about ¼. The boundary-layer technique yielded a slightly more accurate solution to the differential equations obtained for the rectangular cross section than for equations (41) which arise for the triangular and diamond cross sections. Thus the results of the variational method for the triangular and diamond cross sections are probably not quite as accurate as for the rectangular cross section. It appears that for slender cross sections (small values of t_0/c) the variational method is more accurate for large values of K and the Rayleigh-Ritz method is more accurate for small values of K.

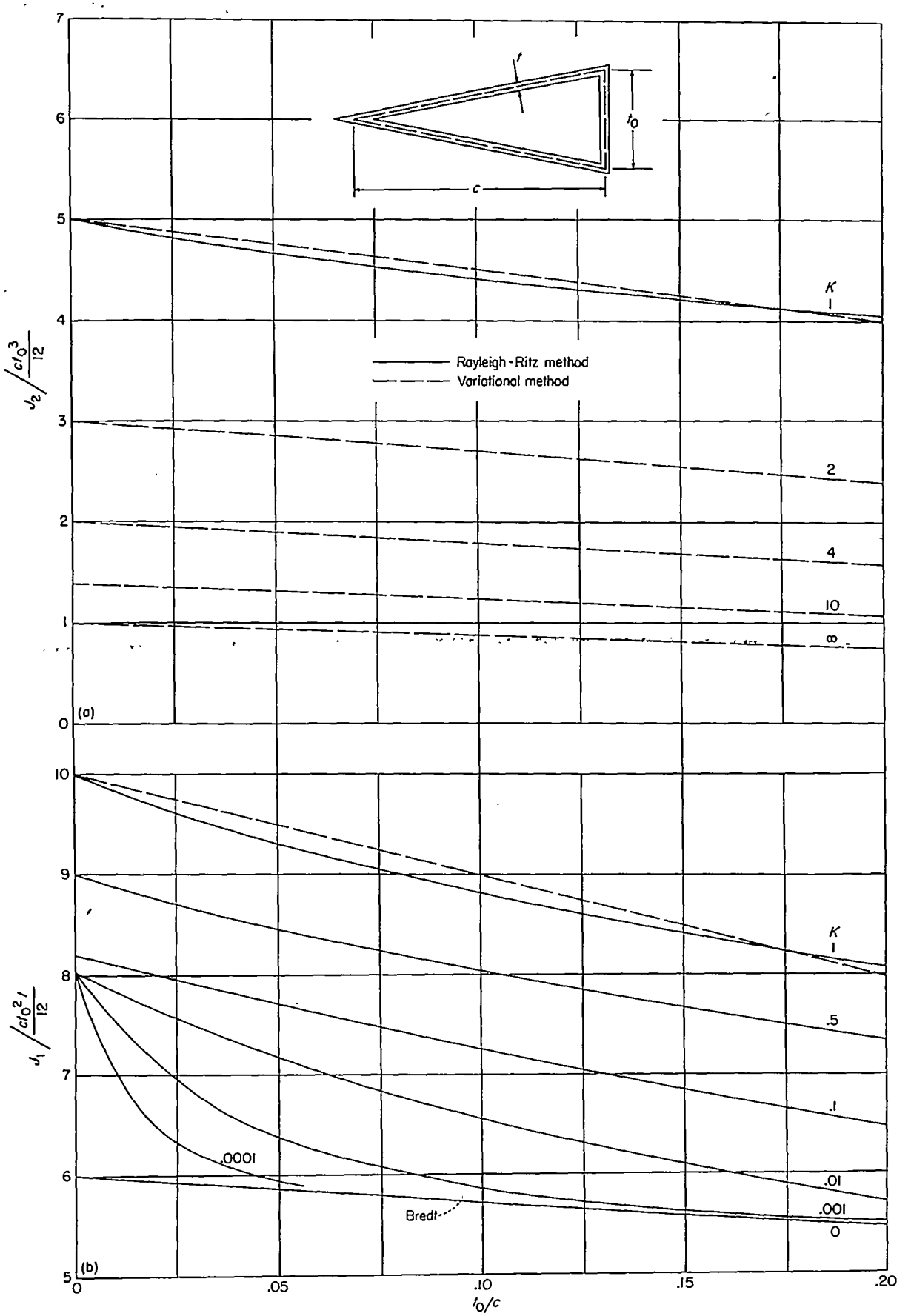

(a) Constant associated with shear modulus of core material.
(b) Constant associated with shear modulus of shell-wall material.

FIGURE 7.—Torsional stiffness constants for a composite thin-walled cylindrical shell of slender triangular cross section.

$$M/\theta = G_1 J_1 = G_2 J_2;\ K = \frac{G_2 \frac{t_0}{2}}{G_1 t}$$

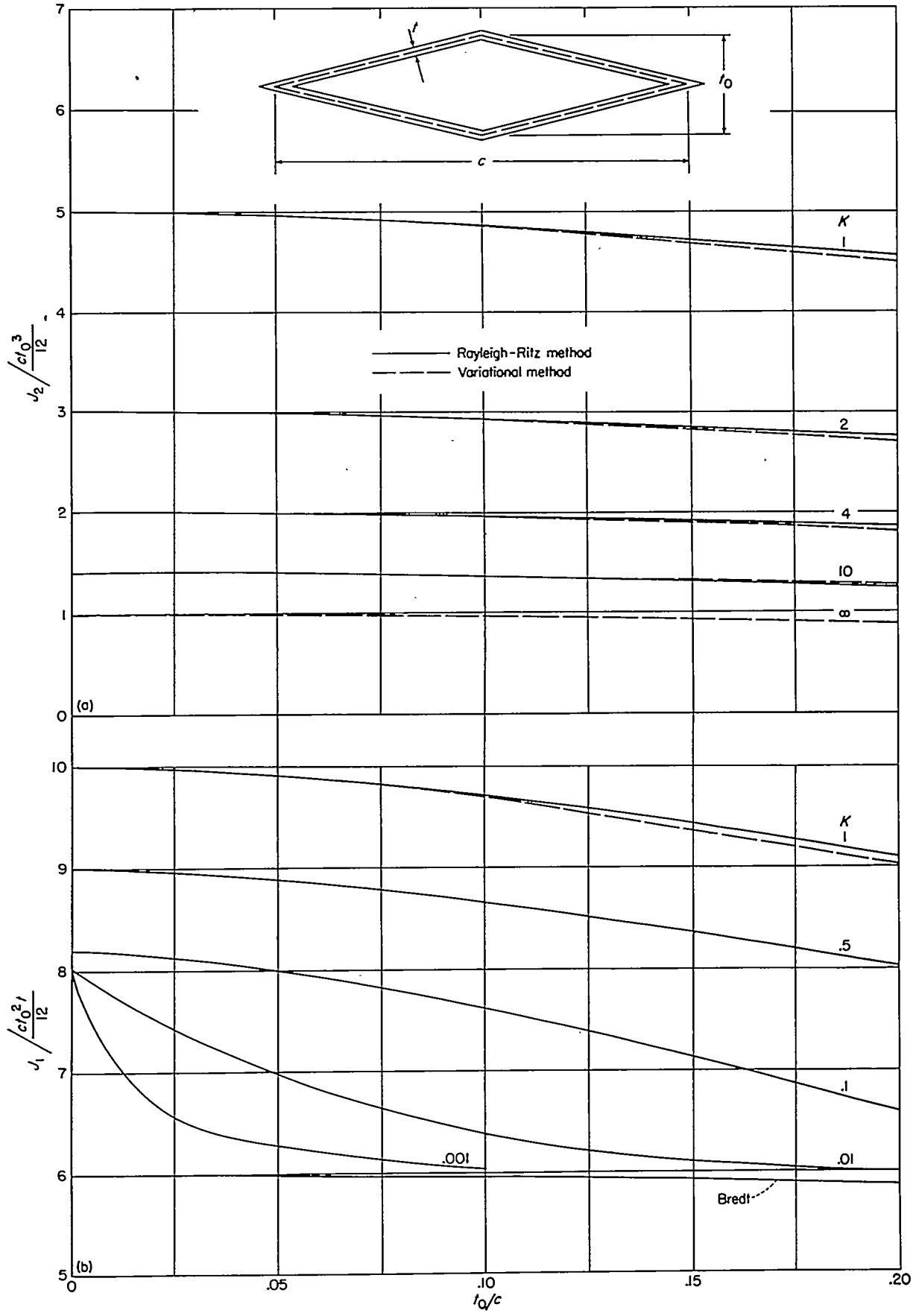

(a) Constant associated with shear modulus of core material.
(b) Constant associated with shear modulus of shell-wall material.

FIGURE 8.—Torsional stiffness constants for a composite thin-walled cylindrical shell of slender diamond cross section.

$$M/\theta = G_1 J_1 = G_2 J_2;\ K = \frac{G_2 \frac{t_0}{2}}{G_1 t}$$

In figures 7 and 8 the solid curves are results of the five-parameter Rayleigh-Ritz method, and the dashed curves show results of the variational method. The Rayleigh-Ritz method certainly leads to a lower bound for the torsional stiffness. The variational approach also leads to a lower bound provided the boundary-layer technique yields a sufficiently accurate solution to equations (41). From the results on the rectangular cross section it appears reasonable to assume that for $K \geqq 1$ the variational method probably gives a lower bound. Therefore, for any particular case where $K \geqq 1$, the higher of the two values of torsional stiffness calculated by the two approximate methods is the more accurate.

REMARKS ON AN ELEMENTARY CALCULATION

It is conceivable that a first approximation to the stiffness of a foam-filled shell could be made simply by adding the torsional stiffness of the core alone to that of the shell alone and neglecting the stiffening effect which results from bonding the core and shell together. Calculations were made by this elementary procedure and the results are shown in figure 9. The ratio $\frac{J_{1,\,\mathrm{elem}}}{J_{1,\,\mathrm{th}}}$ is the ratio of J_1 as calculated by the elementary procedure (neglecting the bonding effect) to J_1 as calculated by the theory of this report. It is seen that for the rectangular cross section the result of the elementary calculation is never more than 5 percent lower than the exact solution. For the triangular and diamond cross sections, however, the elementary procedure does not lead to such good results, and the discrepancy can be as much as 25 percent.

CONCLUDING REMARKS

An approximate boundary-value problem is set up for the Saint-Venant torsion of cylindrical thin-walled shells bonded to a core which fills the interior of the shell and which is made of a material different from that of the shell wall. Solutions for the torsional stiffness are obtained for three particular cross-sectional shapes—an exact solution to the boundary-value problem for rectangular cross sections and approximate solutions for slender triangular and slender diamond cross sections. The approximate solutions are obtained by the use of two energy procedures. These methods may be applicable to other cross sections of practical interest. The choice of approximate method for any particular problem depends on the range of parameters involved.

The stiffness obtained by the simple procedure of adding together the individual stiffnesses of the core and the hollow shell (neglecting the effect of the bond) yields results less than five percent low for rectangular cross sections. For slender triangular and diamond cross sections this elementary approximation is generally not so good and in certain cases it yields results which are considerably low.

LANGLEY AERONAUTICAL LABORATORY,
NATIONAL ADVISORY COMMITTEE FOR AERONAUTICS,
LANGLEY FIELD, VA., *June 7, 1956*.

REFERENCES

1. Payne, L. E.: Torsion of Composite Sections. Iowa State College Jour. Sci., vol. 23, 1949, pp. 381–395.
2. Muskhelishvili, N. I. (Radok, J. R. M., Trans.): Some Basic Problems of the Mathematical Theory of Elasticity. Third ed., P. Noordhoff, Ltd. (Groningen, Holland), 1953, pp. 597–613.
3. Timoshenko, S., and Goodier, J. N.: Theory of Elasticity. Second ed., McGraw-Hill Book Co., Inc., 1951, pp. 278, 298–302.
4. Courant, R.: Variational Methods for the Solution of Problems of Equilibrium and Vibrations. Bull. Am. Math. Soc., vol. 49, Jan. 1943, pp. 1–23.
5. Carrier, G. F.: Boundary Layer Problems in Applied Mechanics. Vol. III of Advances in Applied Mechanics, Richard von Mises and Theodore von Kármán, eds., Academic Press, Inc. (New York), 1953, pp. 1–19.

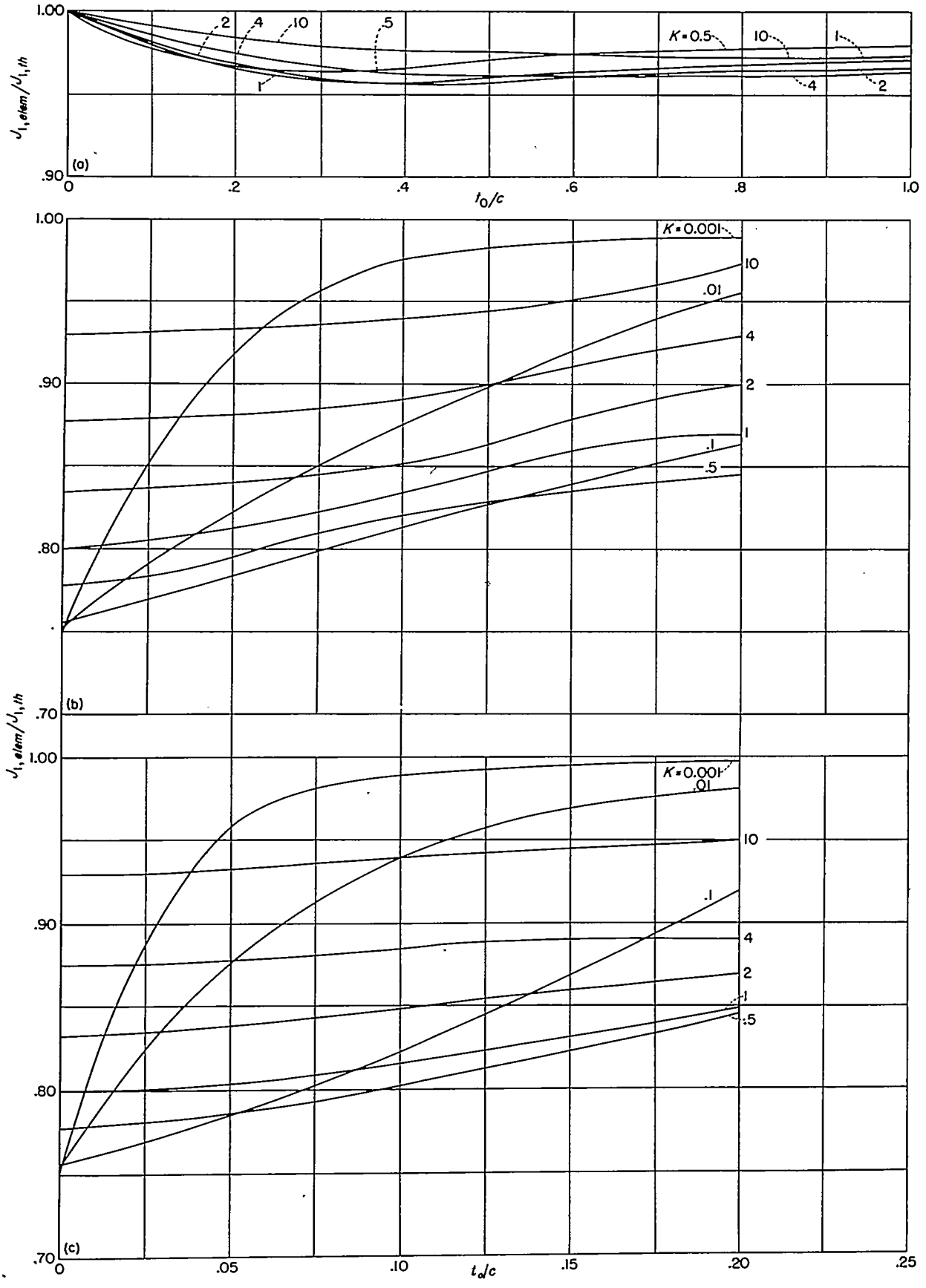

(a) Rectangular cross section.
(b) Triangular cross section.
(c) Diamond cross section.

FIGURE 9.—Comparison between the results for the torsional stiffness constant J_1 obtained from an elementary calculation and the present theory.